

# Naringenin Sensitizes Lung Cancer NCI-H23 Cells to Radiation by Downregulation of Akt Expression and Metastasis while Promoting Apoptosis

Taranga Jyoti Baruah, Kimrose Hauneihkim, Lakhon Kma

Department of Biochemistry, North-Eastern Hill University, Shillong, Meghalaya, India

Submitted: 24-Dec-2019

Revised: 05-Feb-2020

Accepted: 27-May-2020

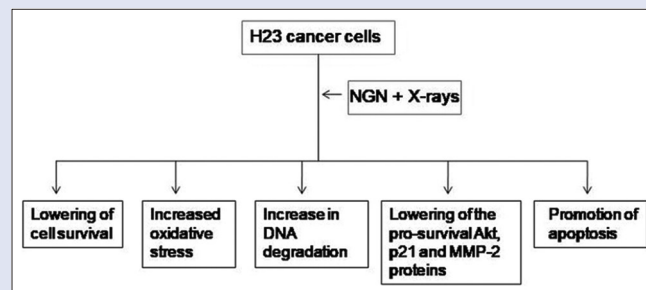
Published: 28-Aug-2020

## ABSTRACT

**Background:** Naringenin (NGN) is a flavonoid that has shown anticancer activities, but the ability of NGN to radiosensitize cells of the non-small cell variety of lung cancer has not been looked into yet. **Objectives:** The objective of the study was to check for the ability of NGN to promote radiosensitization of the lung cancer cell line – NCI-H23 (H23). **Materials and Methods:** 3-(4,5-dimethylthiazol-2-yl)-2,5-diphenyltetrazolium bromide assay, trypan blue exclusion assay, and colony-forming assay were performed to check the effect of NGN, with and without X-ray treatment, on the viability of cancer cells. Protein carbonylation, DNA fragmentation, and caspase-3 activity were determined. The levels of pAkt, Akt, matrix metalloproteinase-2 (MMP-2), RAD50, and p21 proteins were looked at by Western blotting. Messenger RNA (mRNA) levels of AKT1, CASPASE3, BAX, BCL2, and BCLXL were also checked. **Results:** When combined with radiation, NGN lowered the survivability of H23 cells. NGN showed a prooxidant effect while no DNA fragmentation was observed. mRNA levels of CASPASE3 and caspase-3 activity also showed an increase. pAkt, Akt, MMP-2, and p21 protein levels were lowered in the NGN-treated groups, while the RAD50 protein levels showed an increase. The mRNA levels of BCL2 and BCLXL were lowered, while BAX mRNA levels were elevated in response to NGN treatment. **Conclusion:** The results showed that NGN, used singularly or in combination with radiation, can lower the procancerous and prometastatic Akt, p21, and MMP-2 proteins while upregulating the apoptotic process. **Key words:** Akt, caspase-3, matrix metalloproteinase-2, non-small cell lung cancer, naringenin, radiosensitization

## SUMMARY

- Naringenin (NGN) showed potential as a radiosensitizer as it was able to lower cell survival, increase DNA degradation, lower pro-survival proteins, and promote an apoptotic environment in H23 cells. As such NGN deserves to be further investigated *in vivo* as a radiosensitizer.



**Abbreviations used:** NGN: Naringenin; NSCLC: Nonsmall cell lung cancer; MMP-2: Matrix metalloproteinase-2; MRN: Mre11-Rad50-Nbs1; MTT: 3-(4,5-dimethylthiazol-2-yl)-2,5-diphenyltetrazolium bromide; Bcl-2: B cell lymphoma 2; Bcl-XL: B cell lymphoma-extra large; NFκB: Nuclear factor kappa B; Bax: BCL2 associated X; DEVD-pNA: n-acetyl-aspartate-glutamate-valine-aspartate-para-nitroaniline; BCIP/NBT: 5-Bromo-4-chloro-3-indolyl phosphate/nitroblue tetrazolium; ACTB: Actin beta; EGFR: Epidermal growth factor receptor.

## Correspondence:

Dr. Taranga Jyoti Baruah,  
Department of Biochemistry,  
North-Eastern Hill University,  
Cancer and Radiation Countermeasures Unit,  
Shillong - 793 022, Meghalaya, India.  
E-mail: taranga18@gmail.com  
**DOI:** 10.4103/jpm.pm\_535\_19

## Access this article online

Website: [www.phcog.com](http://www.phcog.com)

## Quick Response Code:



## INTRODUCTION

Of all the major types of cancer, lung cancer has consistently scored the highest both in terms of incidence and cancer-related deaths.<sup>[1]</sup> Based on histology, lung cancer can be divided into small cell lung cancer (SCLC) and non-SCLC (NSCLC) with NSCLC contributing to approximately 85% of the lung cancer cases and is also the highest contributor to cancer-related deaths in many countries.<sup>[2,3]</sup> Radiotherapy and chemoradiotherapy form a major part of the treatment modalities for NSCLC.<sup>[4]</sup> The current 5-year survival rate of 5% to 15% clearly demonstrates the resistance of NSCLC to the treatment methods and also the need to look for better treatment alternatives.<sup>[5]</sup>

Akt acts as an oncogene, and high levels of phosphorylated Akt have been reported in most cancers.<sup>[6]</sup> Akt protein is a major mediator of the actions of the PI3K pathway and is often over expressed in most cases of NSCLC.<sup>[7]</sup> In cancer cells that lack a wild-type PTEN, Akt is critical in promoting ionizing radiation-induced metastasis by increasing the expression of matrix metalloproteinase-2 (MMP-2) which often

leads to resistance of cancer cells to radiation therapy.<sup>[8]</sup> The cell cycle regulatory protein cyclin-dependent kinase inhibitor/p21<sup>CIP1/WAF1</sup> (p21) is also known to promote tumor invasiveness and aggressiveness in a p53-deficient environment and is often upregulated in cancer.<sup>[9]</sup> Akt phosphorylates p21 at Ser145 and Thr146 which not only prevents p21 from carrying out the p21-mediated cell cycle arrest but also promotes the inhibition of apoptosis by p21.<sup>[10]</sup> RAD50 is a DNA damage sensor and is a component of the Mre11–Rad50–Nbs1 (MRN) DNA repair

This is an open access journal, and articles are distributed under the terms of the Creative Commons Attribution-NonCommercial-ShareAlike 4.0 License, which allows others to remix, tweak, and build upon the work non-commercially, as long as appropriate credit is given and the new creations are licensed under the identical terms.

**For reprints contact:** [reprints@medknow.com](mailto:reprints@medknow.com)

**Cite this article as:** Baruah TJ, Hauneihkim K, Kma L. Naringenin sensitizes lung cancer NCI-H23 cells to radiation by downregulation of Akt expression and metastasis while promoting apoptosis. *Phcog Mag* 2020;16:S229-35.

complex.<sup>[11]</sup> MRN complex can also promote a p53 independent apoptosis upon severe DNA damage.<sup>[12]</sup> Akt promotes the expression and activity of the antiapoptotic B cell lymphoma 2 (Bcl-2) proteins like B-cell lymphoma 2 (Bcl-2) and B cell lymphoma-extra large via the activation of nuclear factor kappa B (NFκB) while inhibiting the expression and activity of the proapoptotic Bcl-2 proteins, such as BCL2 associated X (Bax) and caspases via inactivating the forkhead family of transcription factors.<sup>[13]</sup>

A lot of effort is now being invested in finding safer and effective compounds which can address the issue of overactivation of Akt in NSCLC cases and along with lowering the radiation resistance of NSCLC. Several plant polyphenols with proven anticancer properties are also currently being investigated as radiosensitisers, as they have been reported to lower the pro-survival proteins such as Akt and NFκB. Examples include quercetin and vicenin-2.<sup>[14,15]</sup> In this study, we check if the commonly available flavonoid, naringenin, can inhibit the activities of Akt and promote the radiosensitization of the NSCLC cell line H23.

## MATERIALS AND METHODS

### Cell culturing

NSCLC cell line H23 was obtained from National Centre of Cell Science, Pune, India, and cultured in a media made up of RPMI 1640 (Invitrogen, USA), 2 mM L-glutamine (Invitrogen, USA), 10% fetal bovine serum (FBS) (HiMedia, India), and 0.1% antibiotics (Invitrogen, USA). HEK293T embryonic cell line was also obtained from the same supplier and cultured in a media consisting of Dulbecco's Modified Eagle Medium (DMEM) (Invitrogen, USA), 1% nonessential amino acids (Invitrogen, USA), 2 mM L-glutamine, 10% FBS, and 0.1% antibiotics.

### Cytotoxicity assay

H23 cells were plated in a 96-well plate at a density of  $1 \times 10^4$  cells per well. Once the cells were attached, they were treated with varying concentrations of naringenin (NGN) (Sigma, USA). NGN was initially dissolved in dimethyl sulfoxide (DMSO) then diluted with RPMI before treating the cells with NGN. 5 mg of 3-(4,5-dimethylthiazol-2-yl)-2,5-diphenyltetrazolium bromide (MTT) (Sigma, USA) was added to 1 ml of phosphate-buffered saline, and 20 μL of the MTT solution was added per well after 24 h of adding NGN. MTT allowed color formation, and the intensity of the color formed was read by measuring absorbance at 595 nm using a microplate reader (Bio-Rad, USA).

### Proliferation assay

H23 cells were given three sets of treatments: treated with NGN alone and treated with X-radiation at a dose rate of 1 Gy/min for a period of 2, 4, 6, and 8 min respectively, thereby totaling to doses of 2, 4, 6, and 8 Gy, respectively. In the third group, the treatment with NGN was followed by a treatment with the same pattern of X-rays doses as in the previous case (combination group). Another group of cells were kept untreated and served as the control. Cells in the NGN alone and the combination group of NGN and radiation were treated with NGN for 24 h, while in the control and radiation alone group, the cells were treated with RPMI + 0.01% DMSO. After 24 h, the cells in the radiation alone group and combination group were subjected to X-irradiation (Faxitron, USA). Thereafter, the media was discarded from all the groups and fresh media was added and kept in the incubator for 24 h. Once the treatment period was over, the MTT solution was added and the readings were taken at 595 nm.

### HEK293T cell viability assay

HEK293T cells were plated in a 6-well plate with a plating density of  $2 \times 10^5$  cells per well. The HEK293T cells were treated in the same manner as the H23 cancer cells. This was followed by dispersing the adherent cells via trypsinization, and a count of the viable trypan blue-stained cells was achieved using a chambered hemocytometer (HBG, Germany) by viewing in an inverted microscope.

### H23 cell viability assay

Based on the results of the above three experiments, the cell viability assay, and the remainder of the experiments, the H23 cells were irradiated with only 6 Gy dose of X-rays in the radiation alone and combination group. The combination group was pretreated with NGN. Another set of cells was treated with NGN alone and there was a set of untreated control cells. This was followed by dispersing the adherent cells via trypsinization, and a count of the trypan blue-stained cells was achieved using a chambered hemocytometer (HBG, Germany) by viewing in an inverted microscope. Cells whose cytoplasm was clear with a ring of blue stain on the membrane were considered to be viable and cells without a clear cytoplasm and a distorted membrane were considered as dead.<sup>[16]</sup>

### Clonogenic assay

The clonogenic assay was performed according to the steps mentioned by Crowley *et al.*<sup>[17]</sup> with slight modifications. Once the treatment process of the cells was over, the cells were dispersed via trypsinization and plated on a 24-well plate with a density of 200 cells per well and grown for 2 weeks. On the 14<sup>th</sup> day, methanol was applied on the cells to fix the cells, followed by staining with 0.5% crystal violet, after which a colony count was taken under a microscope.

### Protein carbonylation assay

The protocol described by Colombo *et al.*<sup>[18]</sup> was followed for checking the levels of carbonylated proteins, with minor modifications. Once the treatment period was over, cells were lysed and 10 mM 2,4-dinitrophenylhydrazine (DNPH) was added to the lysates, after which they were kept in the dark for an hour. Trichloroacetic acid (TCA) solutions of strengths 20% followed by 10% were added to the lysate-DNPH mixture with centrifuging after each addition of TCA at 11000 g for 5 min. An equimolar solution of ethyl acetate and ethanol was then added to the pellet obtained and again was centrifuged with the same parameters. The supernatant was discarded and the pellet was resuspended in guanidine hydrochloride solution of strength 6 M. Readings of absorbance were taken at a wavelength of 366 nm using a spectrophotometer.

### DNA fragmentation assay

Isolation of DNA was achieved by making minor adjustments of the protocol mentioned in Saadat *et al.*'s study.<sup>[19]</sup> After the lysis of H23 cells, the lysates were treated with chloroform: isoamyl alcohol, and the aqueous upper phase was separated by spinning the mixture at 12,000 g for a duration of 5 min. An equal volume of the cold isopropanol was added to the isolated aqueous phase and the DNA was pelleted from this mixture by centrifuging at the same parameters as earlier. This was followed by drying and subsequent dissolving of the pellet in Tris-EDTA (TE) buffer. Electrophoresis of the DNA was performed on a 1.5% agarose gel at a voltage setting of 70V. Ethidium bromide was used at a strength of 0.3 μg/ml to stain the DNA followed by viewing under a gel doc (Bio-Rad, USA).

## DEVDase assay

This assay was performed to estimate caspase-3 activity as per the instructions available in the protocol booklet of the manufacturer of the assay kit (ABCAM, UK). Cytosolic extracts were incubated in substrate buffer containing caspase-3 substrate n-acetyl-aspartate-glutamate-valine-aspartate-para-nitroaniline for a period of 4 h at 37°C, which was followed by spectrophotometric readings taken at 400 nm. An increase in caspase-3 activity was compared with the control set and expressed in terms of fold change.

## Western blotting analysis

For performing Western blotting, total proteins were isolated by lysing the H23 cells. The Bradford reagent was used to ascertain the protein content in the cell lysates.<sup>[20]</sup> Equal amounts of proteins were loaded and run on an sodium dodecyl sulfate-polyacrylamide gel electrophoresis gel and were transferred into a membrane made of nitrocellulose. Membranes were incubated in rabbit monoclonal antibodies against Akt, Akt with S473 phosphorylation (pAkt), p21, MMP-2, and Rad-50 (ABCAM, UK) proceeded by treating membranes in anti-rabbit secondary antibody conjugated to alkaline phosphatase. Color development of the immunoblot was achieved by treating the membrane with the appropriate substrate.<sup>[21]</sup>

## Gene expression analysis

The messenger RNA (mRNA) levels of AKT1, CASPASE3, BCL2, BCLXL, and BAX genes were measured using a SYBR green based quantitative real time polymerase chain reaction (PCR) kit (Applied Biosystems, USA) using a PCR system with real time applications (Applied Biosystems). Trizol reagent (Sigma, USA) was used to isolate RNA from the cells. The isolated RNA was then used as a template to form the corresponding cDNA using a reverse transcriptase based kit from Applied Biosystems. The cDNA was used to run real-time PCR using an SYBR Green kit. Actin beta was used as the reference gene, and the changes in the expression levels were quantified in relation to the reference gene.<sup>[22]</sup>

## Statistical analysis

The data have been expressed in terms of mean  $\pm$  standard deviation. Significance values were calculated using ANOVA (SPSS, USA) and differences between groups were considered to be statistically significant if  $P < 0.05$ .

## RESULTS

### Naringenin lowers cancer cell survival as a single agent and when naringenin precedes radiation treatment

H23 cell survival showed a gradual lowering with increasing doses of NGN [Figure 1a]. Cell survival was lowered by 50% ( $**P < 0.01$ ) when the NGN dose was increased to 100  $\mu$ M. We checked the effect of treating the H23 cells with 100  $\mu$ M NGN prior to treatment with radiation as compared to treating the cells with radiation alone [Figure 1b]. We observed a significantly lowered cell survival when the H23 cells were treated with NGN prior to radiation treatment with respect to the cells treated with only X-rays ( $**P < 0.01$  vs. 2 Gy, 4 Gy, and 6 Gy irradiated group and  $*P < 0.05$  vs. 8 Gy radiation alone group). In case of the HEK293T embryonic cells, 100  $\mu$ M of NGN did not lower the number of viable HEK293T cells. Between the radiation treated doses, cells in the combination group of NGN + 6 Gy X-radiation showed higher levels of viability in relation to the cells treated only with 6 Gy of X-rays [Figure 1c,  $**P < 0.01$ ]. As observed from the cell proliferation assay [Figure 1b], the combination groups of 8 Gy and 6 Gy had the minimum number of

surviving cells ( $44.28 \pm 3.55$  and  $53.36 \pm 3.39$ , respectively). On the other hand, from the HEK293T viability assay [Figure 1c], we observed that the combination group of 8 Gy had a percent cell viability of  $52.89 \pm 2.75$ , while in the combination group of 6 Gy, the percent cell viability stood at  $84.95 \pm 5.22$ . As NGN acted as a radiosensitizer at 6 Gy while also being radioprotective at the same dose, we decided to proceed with the rest of the study using only the 6 Gy dose of radiation.

We took a count of the viable H23 cells [Figure 1d], and the number of surviving cells in the NGN alone group was observed to be reduced to  $59.35 \pm 3.45$  ( $**P < 0.01$  vs. control) and  $63.17 \pm 3.47$  in the combination group ( $**P < 0.01$  vs. 6 Gy). From Figure 1e, we observed that the dead cell count was increased by fourfolds in both the NGN-treated groups with respect to the control and cells treated with only 6 Gy of X-rays ( $**P < 0.01$  and  $**P < 0.01$ , respectively). The clonogenic assay results [Figure 1f and g] showed a lowering in the number of colonies formed and subsequently a significant lowering of the surviving cell percentage in the NGN-treated groups,  $53.21 \pm 4.78$  in the NGN alone group ( $**P < 0.01$  vs. control) and  $39.18 \pm 3.59$  in the combination group ( $**P < 0.01$  vs. 6 Gy).

### Naringenin increases oxidative stress in H23 cells

NGN caused an increase in the levels of carbonylated proteins when used alone ( $**P < 0.01$ ). The increase in carbonylated proteins was also observed in the radiation-treated groups [Figure 2]. Increase in carbonylated proteins is an indicator of oxidative stress.<sup>[18]</sup>

### Naringenin promoted DNA degradation

Although there was no observable DNA fragmentation in any of the treatment groups [Figure 3a], the increase in the levels of the DNA damage sensing protein RAD50, in the combination group of NGN + 6 Gy radiation ( $*P < 0.05$ ), pointed toward an increased DNA damage in the combination group [Figure 3b and c].

### Naringenin lowers Akt levels and modulates its downstream effectors

pAkt [Figure 4a and b] protein levels showed a reduction in both NGN used alone and when NGN treatment was followed by exposure to X-rays with respect to the control and X-ray alone group ( $**P < 0.01$  vs. control and  $**P < 0.01$  vs. 6 Gy). Akt protein levels [Figure 4a and c] also showed a similar reduction in the NGN-treated groups of NGN and NGN + 6 Gy in relation to the control and X-ray alone group ( $**P < 0.01$  and  $*P < 0.05$ , respectively). The gene expression levels of AKT1 gene [Figure 4f] showed a significant lowering in the NGN-treated group with respect to the control ( $**P < 0.01$ ) and also in the combined treatment group of NGN + 6 Gy with respect to the 6 Gy-treated cells ( $**P < 0.01$ ). The p21 levels [Figure 4a and d] were lowered in the NGN alone group in relation to the control ( $*P < 0.05$ ) and in the combination group in relation to the 6 Gy group ( $**P < 0.01$ ). The MMP-2 levels were lowered in both the NGN-treated groups, NGN alone and NGN + 6 Gy, with respect to the control and 6 Gy groups, respectively. ( $**P < 0.01$  vs. control and  $**P < 0.01$  vs. 6 Gy, respectively).

### Naringenin treatment promoted apoptosis in H23 cells

The mRNA levels of the antiapoptotic BCL2 gene [Figure 5a] was downregulated in the NGN + 6 Gy group ( $**P < 0.01$  vs. 6 Gy). BCLXL mRNA levels were also lowered in the combination group of NGN + 6 Gy in relation to the 6 Gy-treated cells ( $*P < 0.05$ ). The proapoptotic BAX mRNA levels [Figure 5c] were increased by NGN both when it was used alone ( $*P < 0.05$ ) and when it was combined with 6 Gy radiation ( $**P < 0.01$ ). NGN increased the CASPASE3 mRNA levels [Figure 5d] when used alone ( $*P < 0.05$ ), while no statistically



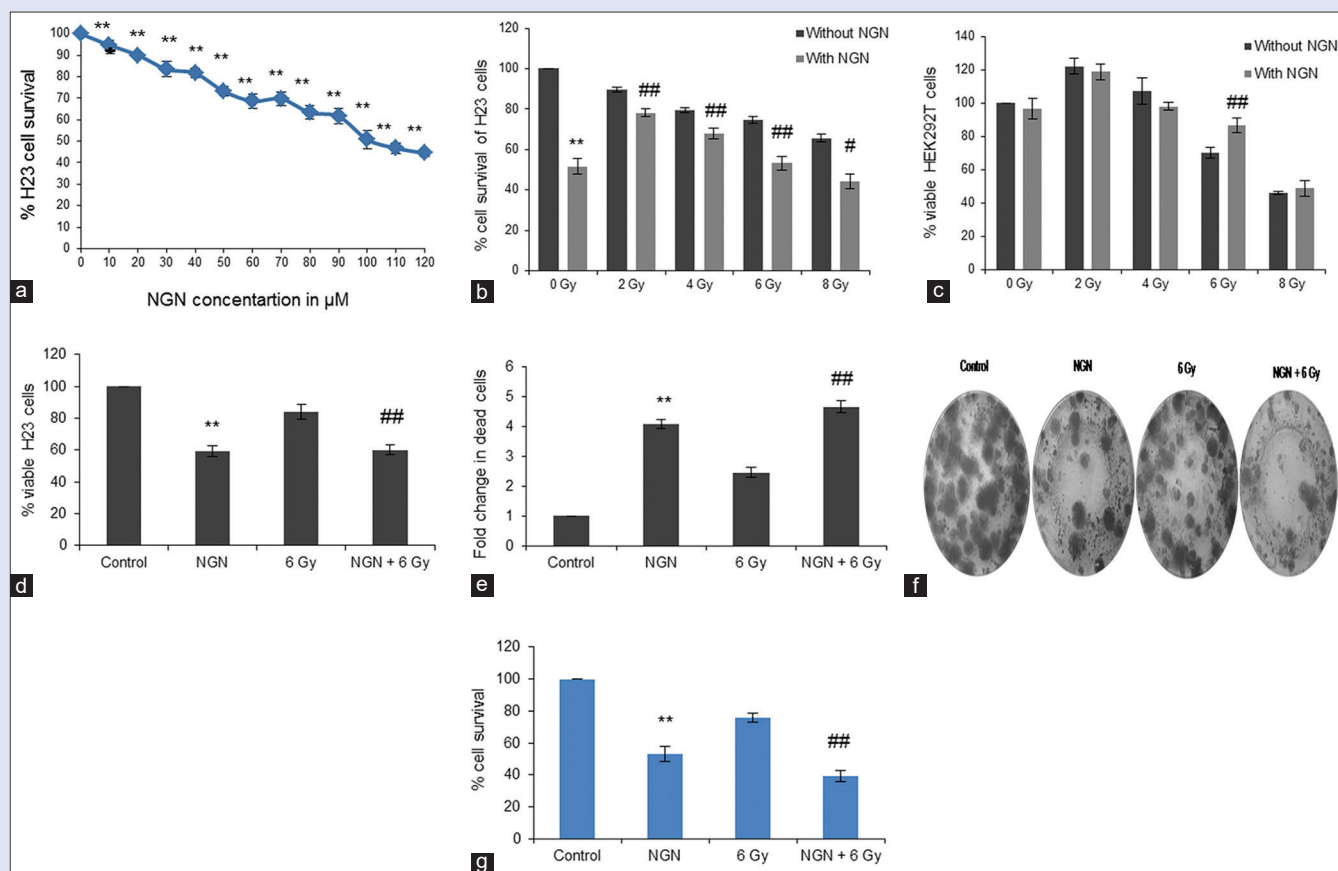


**Figure 1:** Naringenin lowers H23 cell survival singularly and in combination with radiation. (a) Graph showing the percent cell survival of H23 cells with increasing doses of naringenin.  $**P < 0.01$  versus control. (b) Graph showing percent cancer cell survival under various treatment groups.  $**P < 0.01$  versus control and  $^{##}P < 0.01$  versus 2 Gy, 4 Gy and 6 Gy irradiated group, while  $^{*}P < 0.05$  versus 8 Gy irradiation alone group. (c) Bar graph for percent cell survival of normal fibroblast cells under various treatment groups.  $^{**}P < 0.01$  versus the respective irradiated group. (d) Bar graph showing percent viable H23 cells after various treatments.  $**P < 0.01$  versus control and  $^{##}P < 0.01$  versus respective irradiated group. (e) Bar graph showing fold change in dead H23 cells after various treatments.  $**P < 0.001$  versus control and  $^{##}P < 0.01$  versus respective irradiated group. (f) H23 colonies after staining with crystal violet. (g) Bar graph showing percent surviving cells from colony forming assay.  $**P < 0.01$  versus control and  $^{##}P < 0.01$  versus respective irradiated group. All values are expressed as mean  $\pm$  standard deviation. (Figure Legend 1 to be reproduced at full page width)

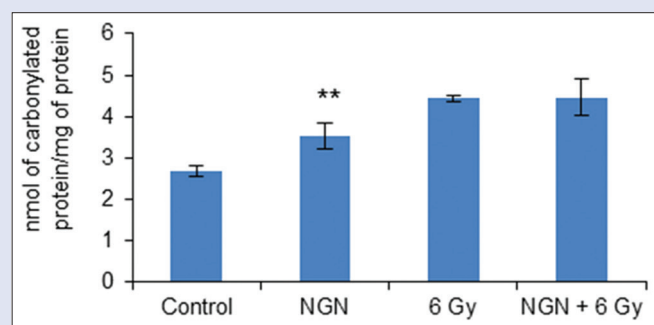


**Figure 2:** Bar graph showing nmol of carbonylated protein per mg of protein after various treatments.  $**P < 0.01$  versus control. Values are mean  $\pm$  standard deviation. (Figure legend 2 to be reproduced at full page width)

significant difference in the levels of CASPASE3 mRNA in the radiation-treated groups was observed. There was an approximately 2 fold increase in the activity of caspase-3 [Figure 5e] in the NGN alone

group ( $^{*}P < 0.05$  vs. control) and when NGN treatment preceded radiation treatment ( $^{##}P < 0.01$  vs. 6 Gy).

## DISCUSSION

The results from the cytotoxicity and proliferation assays of H23 cells showed that NGN was able to lower the survivability of the H23 cells both alone and in combination with radiation [Figure 1a and b]. At the same time, we observed a potential radioprotective effect of NGN on the HEK293T embryonic cells, as evidenced by a higher count of viable cells in the combination groups [Figure 1c]. We also observed a reduction in the viable cancer cell count, while the dead cell count showed an increase in the NGN-treated groups which further showed the chemotherapeutic and radiosensitizing potential of NGN upon the H23 cell line [Figure 1d and e]. We performed a colony-forming assay [Figure 1f] to further confirm our results and to account for the delayed membrane breakage shown by cells in response to treatment or by cells entering a cell cycle delay in response to treatment which could affect the results of the trypan blue and MTT assays.<sup>[23]</sup> Calculating the percent cell survival from the number of colonies formed, we observed that the reduction in the number of surviving

cancer cells was observed in both the cases involving treatment with NGN [Figure 1g].

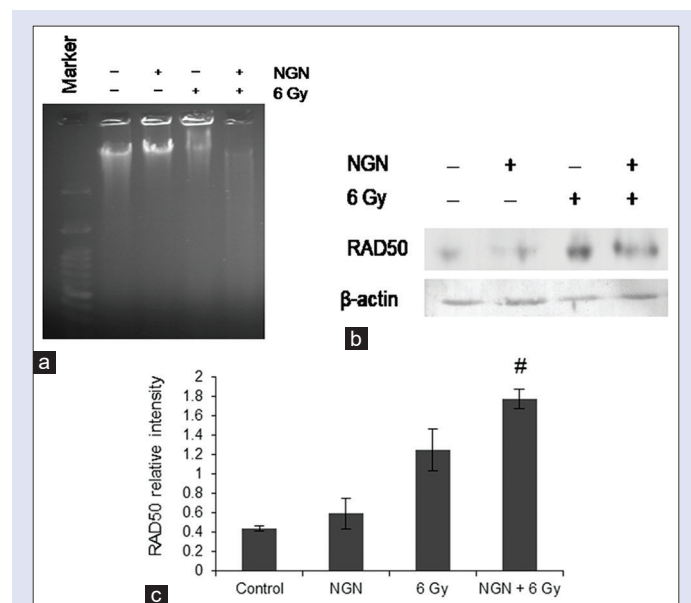


**Figure 3:** Naringenin and DNA damage. (a) naringenin in combination with radiation promotes DNA degradation. (b) Western blot analysis of Rad50 protein. (c) Bar graph showing the densitometric plot of the level of Rad50 protein. \* $P < 0.05$  versus respective irradiated group. Values are expressed as mean  $\pm$  standard deviation. (Figure Legend 3 to be reproduced at full page width)

The increase in carbonylated proteins in the NGN-treated groups showed the ability of NGN to act as a pro-oxidant [Figure 2]. Phytochemicals have been reported to exert their pro-oxidant effects via increased protein carbonylation; for example, green tea polyphenols cause an increase in the carbonylated proteins.<sup>[24]</sup> Proanthocyanidins also exert their proapoptotic effect on human adenocarcinoma cells via increasing protein carbonylation.<sup>[25]</sup> The lowering of Akt levels in the NGN-treated groups can also contribute to increased oxidative stress, as Akt is critical in the maintenance of redox homeostasis.<sup>[26]</sup>

We observed no fragmentation of DNA in any of the treated groups [Figure 3a]. The lack of fragmentation can be attributed to the very low levels of the caspase-activated DNase (CAD) protein in lung tissues and also in adenocarcinomas, which is responsible for carrying out the fragmentation of the DNA.<sup>[27,28]</sup> The increased levels of the DNA damage sensing RAD50 protein,<sup>[11]</sup> especially in the combination group of NGN + 6 Gy, indicated the presence of DNA damage in the H23 cancer cells [Figure 3b and c]. Rad50 also has pro-apoptotic activities and increases in the levels of Rad50 have been associated with increased apoptosis in cancer cells. Flavonoids promote the levels of Rad50 protein to induce apoptotic cell death in cancer cells.<sup>[29]</sup> The lowering of H23 cell survival in the combination group and the upregulation of caspase-3 activity is an indicator of increased apoptotic activity, ultimately leading to cell death.

There was a lowering of pAkt [Figure 4a and b] and Akt [Figure 4a and c] proteins and AKT1 mRNA [Figure 4f] in the NGN-treated groups. The lowering of Akt levels could be attributed to the reported ability of NGN to lower the expression and activity of upstream receptor kinases like epidermal growth factor receptor which is known to activate Akt.<sup>[30,31]</sup> The lowering of p21 was observed in the NGN-treated groups [Figure 4a and d]. The lowering of p21 is significant, as lowering of p21

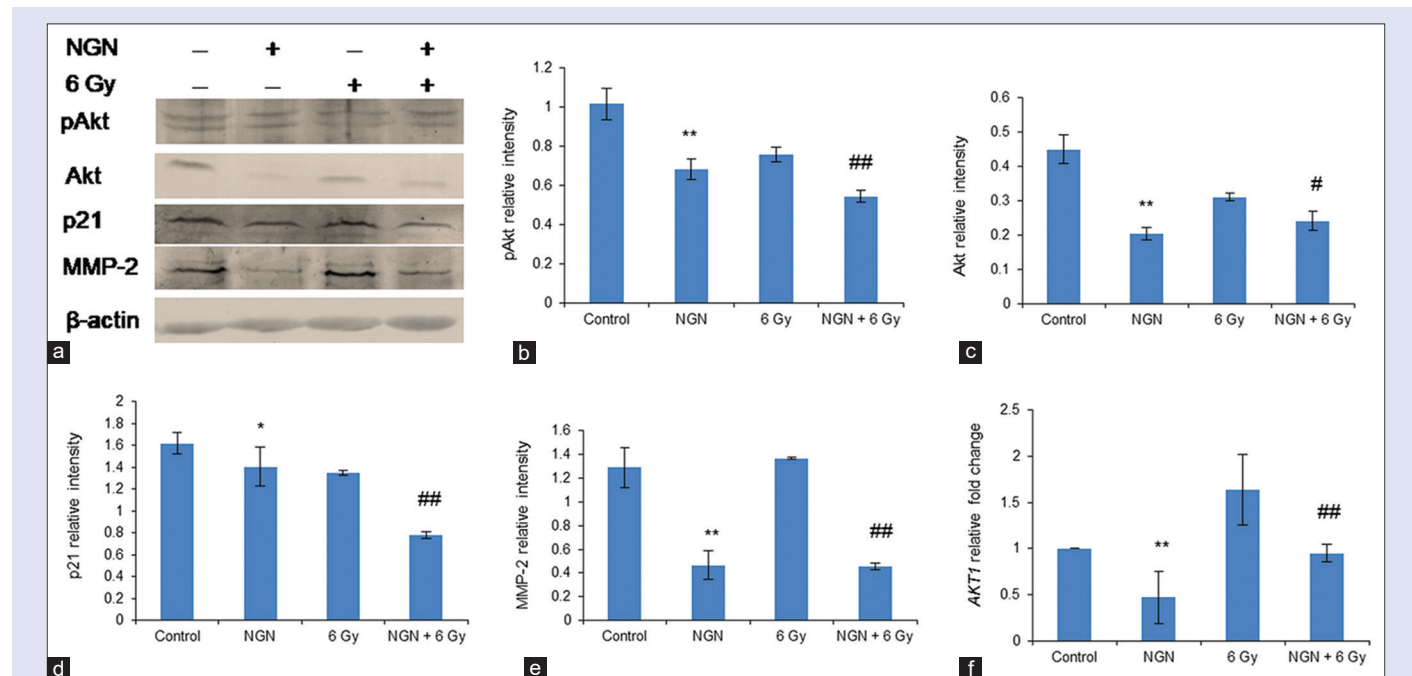


**Figure 4:** Naringenin lowers the expression of pAkt, Akt, p21, and matrix metalloproteinase-2. (a) Western blotting images of pAkt, Akt, p21, and matrix metalloproteinase-2 proteins. Densitometric plots of the level of (b) pAkt protein, \*\* $P < 0.01$  versus control and ## $P < 0.01$  versus respective irradiated group; (c) Akt protein, \*\* $P < 0.01$  versus control and \* $P < 0.05$  versus respective irradiated group; (d) p21 protein, \* $P < 0.05$  versus control and ## $P < 0.01$  versus respective irradiated group; (e) matrix metalloproteinase-2 protein, \*\* $P < 0.01$  versus control and ## $P < 0.01$  versus respective irradiated group. All groups were normalized with  $\beta$ -actin protein. (f) Fold change in messenger RNA expression of AKT1. \*\* $P < 0.01$  versus control and ## $P < 0.01$  versus respective irradiated group. All values are expressed as mean  $\pm$  standard deviation. (Figure legend 4 to be reproduced at full page width)

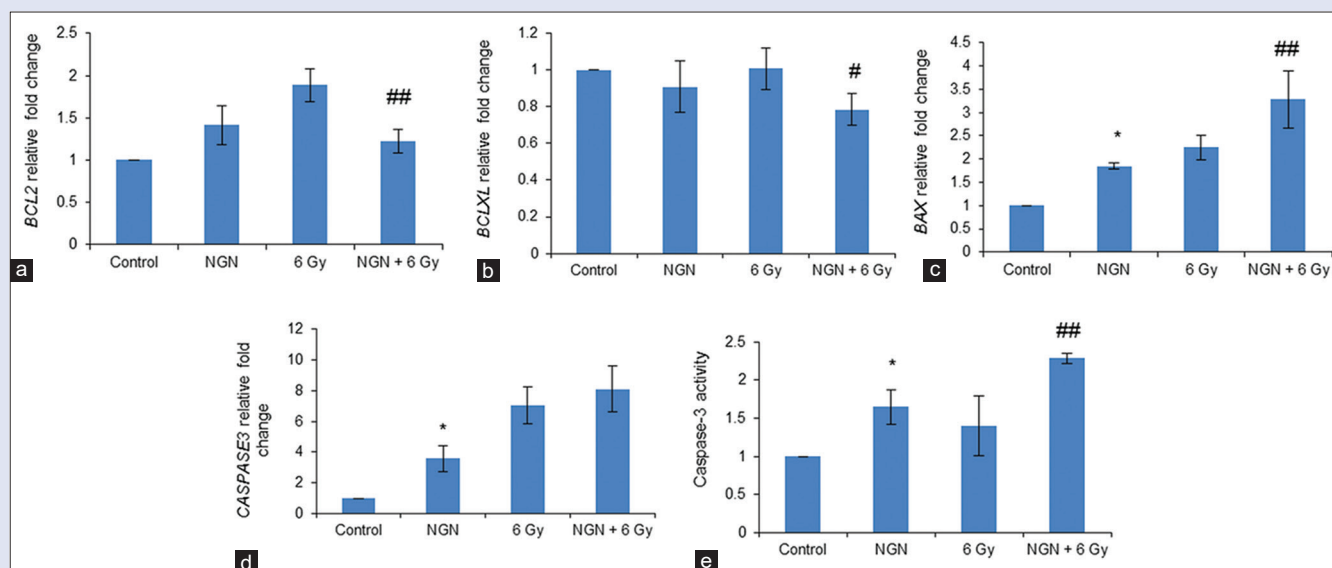


**Figure 5:** Naringenin promotes apoptosis. Fold change in the messenger RNA expression of (a) *BCL2*,  $^{**}P < 0.01$  versus respective irradiated group; (b) *BCLXL*,  $^{*}P < 0.05$  versus respective irradiated group; (c) *BAX*,  $^{*}P < 0.05$  versus control and  $^{**}P < 0.01$  versus respective irradiated group; (d) *CASPASE3*,  $^{*}P < 0.05$  versus control. All values were normalized with *ACTB* endogenous control; (e) graph for fold change in caspase-3 activity,  $^{*}P < 0.05$  versus control and  $^{**}P < 0.01$  versus respective irradiated group. All values are expressed as mean  $\pm$  standard deviation. (Figure Legend 5 to be reproduced at full page width).

has been reported to promote cell death in response to radiation and also promotion of radiation-induced apoptosis.<sup>[32]</sup> There was a reduction in the MMP-2 [Figure 4a and e] levels in both the NGN-treated groups. The lowering of MMP-2 can be attributed to a lowering of Akt, as Akt contributes to increasing the activity of MMP-2.<sup>[8]</sup> The lowering of MMP-2 is associated with lowered metastasis, greater radiosensitivity, and increased apoptosis in NSCLC.<sup>[33,34]</sup>

The gene expression level of the antiapoptotic BCL2 and BCLXL genes [Figure 5a and b] was downregulated in the combination group where NGN was combined with a radiation dose of 6 Gy. The lowering of the expression of these two genes holds importance not only because they code for antiapoptotic proteins but also because these protein products are involved in promoting the Akt pathway.<sup>[35-38]</sup> The proapoptotic BAX gene mRNA levels registered an elevation in both the NGN-treated groups [Figure 5c]. The BAX protein encoded by the BAX gene is a positive prognostic marker for NSCLC and can promote apoptosis in both caspase dependent and independent ways along with promoting radiosensitization.<sup>[39,40]</sup> The activity levels of caspase-3 increased in both the NGN-treated groups [Figure 5e]. The increased activity of caspase-3 in the combination group of NGN + 6 Gy with respect to the 6 Gy radiation group minus any corresponding changes in the CASPASE3 mRNA levels between the radiation treated groups [Figure 5d] can be caused by the observed lowering of Akt and p21 levels, both of which are known to inhibit the activity of a caspase-3 protein.<sup>[41,42]</sup> An increase in caspase-3 activity is also favorable as caspase-3 can also serve as a marker of radiosensitivity.<sup>[43]</sup>

## CONCLUSION

In conclusion, the results from our study show that NGN had a chemotherapeutic and a radiosensitizing effect on the H23 cancer cells. NGN singularly and when combined with a radiation dose of 6 Gy caused a reduction in Akt, MMP-2, and p21 levels and promoted DNA damage. There was a diminishing of the mRNA levels of antiapoptotic BCL2 and BCLXL genes, while an increase in mRNA levels of proapoptotic BAX and CASPASE3 genes was observed in the NGN-treated groups. An

increase in the proteolytic activity of caspase-3 was also observed in the NGN-treated groups. However, our results are based on a single cell line, and we plan to extend our work into other NSCLC cancer models to further validate NGN as a radiosensitizer of NSCLC cells.

## Acknowledgements

The authors would like to thank the Department of Biochemistry, North Eastern Hill University for providing the facilities to carry out the work.

## Financial support and sponsorship

This work was supported by funds provided by the Department of Science and Technology, Science and Engineering Research Board, New Delhi, India, to Dr. L. Kma (SERB/F/3862/2014-15) and grant from University Grants Commission, New Delhi, India, under Departmental Research Support-II and Departmental Research Support-III program to the Department of Biochemistry, NEHU, Shillong, India.

## Conflicts of interest

There are no conflicts of interest.

## REFERENCES

- Jones GS, Baldwin DR. Recent advances in the management of lung cancer. *Clin Med* 2018;18:41-6.
- Arbour KC, Riely GJ. Systemic therapy for locally advanced and metastatic non-small cell lung cancer: A review. *JAMA* 2019;322:764-74.
- Inamura K. Lung cancer: Understanding its molecular pathology and the 2015 WHO classification. *Front Oncol* 2017;7:193.
- Rosenzweig KE, Gomez JE. Concurrent chemotherapy and radiation therapy for inoperable locally advanced non-small-cell lung cancer. *J Clin Oncol* 2017;35:6-10.
- Zeng J, Cai S. Beviscapine suppresses the growth of non-small cell lung cancer by enhancing microRNA-7 expression. *J Biosci* 2017;42:121-9.
- Mundi PS, Sachdev J, McCourt C, Kalinsky K. AKT in cancer: New molecular insights and advances in drug development. *Br J Clin Pharmacol* 2016;82:943-56.
- Crosbie PA, Crosbie EJ, Aspinall-O'Dea M, Walker M, Harrison R, Pernemalm M, *et al.* ERK and AKT phosphorylation status in lung cancer and emphysema using nanocapillary

- isoelectric focusing. *BMJ Open Respir Res* 2016;3:e000114.
8. Park CM, Park MJ, Kwak HJ, Lee HC, Kim MS, Lee SH, *et al.* Ionizing radiation enhances matrix metalloproteinase-2 secretion and invasion of glioma cells through Src/epidermal growth factor receptor-mediated p38/Akt and phosphatidylinositol 3-kinase/Akt signaling pathways. *Cancer Res* 2006;66:8511-9.
  9. Abbas T, Dutta A. p21 in cancer: Intricate networks and multiple activities. *Nat Rev Cancer* 2009;9:400-14.
  10. Li Y, Dowbenko D, Lasky LA. AKT/PKB phosphorylation of p21Cip/WAF1 enhances protein stability of p21Cip/WAF1 and promotes cell survival. *J Biol Chem* 2002;277:11352-61.
  11. Nowsheen S, Yang ES. The intersection between DNA damage response and cell death pathways. *Exp Oncol* 2012;34:243-54.
  12. Stracker TH, Petrini JH. The MRE11 complex: Starting from the ends. *Nat Rev Mol Cell Biol* 2011;12:90-103.
  13. Qian J, Zou Y, Rahman JS, Lu B, Massion PP. Synergy between phosphatidylinositol 3-kinase/Akt pathway and Bcl-xL in the control of apoptosis in adenocarcinoma cells of the lung. *Mol Cancer Ther* 2009;8:101-9.
  14. Malik A, Sultana M, Qazi A, Qazi MH, Parveen G, Waqar S, *et al.* Role of natural radiosensitizers and cancer cell radioresistance: An update. *Anal Cell Pathol (Amst)* 2016;2016:6146595.
  15. Baruah TJ, Kma L. Vicerin-2 acts as a radiosensitizer of the non-small cell lung cancer by lowering Akt expression. *Biofactors* 2019;45:200-10.
  16. Strober W. Trypan blue exclusion test of cell viability. *Curr Protoc Immunol* 2015;111:A3.B.1-3.
  17. Crowley LC, Christensen ME, Waterhouse NJ. Measuring survival of adherent cells with the colony forming assay. *Cold Spring Harb Protoc* 2016;2016:721-4.
  18. Colombo G, Clerici M, Garavaglia ME, Giustarini D, Rossi R, Milzani A, *et al.* A step-by-step protocol for assaying protein carbonylation in biological samples. *J Chromatogr B Analyt Technol Biomed Life Sci* 2016;1019:178-90.
  19. Saadat YR, Saeidi N, Vahed SZ, Barzegari A, Barar J. An update to DNA ladder assay for apoptosis detection. *Bioimpacts* 2015;5:25-8.
  20. Bradford MM. A rapid and sensitive method for the quantitation of microgram quantities of protein utilizing the principle of protein-dye binding. *Anal Biochem* 1976;72:248-54.
  21. Kma L, Sharan RN. Dimethylnitrosamine-induced reduction in the level of poly-ADP-ribosylation of histone proteins of blood lymphocytes – A sensitive and reliable biomarker for early detection of cancer. *Asian Pac J Cancer Prev* 2014;15:6429-36.
  22. Livak KJ, Schmittgen TD. Analysis of relative gene expression data using real-time quantitative PCR and the 2<sup>-</sup>(Delta Delta C(T)) Method. *Methods* 2001;25:402-8.
  23. Weisenthal LM, Dill PL, Kurnick NB, Lippman ME. Comparison of dye exclusion assays with a clonogenic assay in the determination of drug-induced cytotoxicity. *Cancer Res* 1983;43:258-64.
  24. Madian AG, Myracle AD, Diaz-Maldonado N, Rochelle NS, Janle EM, Regnier FE. Determining the effects of antioxidants on oxidative stress induced carbonylation of proteins. *Anal Chem* 2011;83:9328-36.
  25. Chung WG, Miranda CL, Stevens JF, Maier CS. Hop proanthocyanidins induce apoptosis, protein carbonylation, and cytoskeleton disorganization in human colorectal adenocarcinoma cells via reactive oxygen species. *Food Chem Toxicol* 2009;47:827-36.
  26. Koundouros N, Poulgiannis G. Phosphoinositide 3-kinase/akt signaling and redox metabolism in cancer. *Front Oncol* 2018;8:160.
  27. Mukae N, Enari M, Sakahira H, Fukuda Y, Inazawa J, Toh H, *et al.* Molecular cloning and characterization of human caspase-activated DNase. *Proc Natl Acad Sci U S A* 1998;95:9123-8.
  28. Errami Y, Brim H, Oumouna-Benachour K, Oumouna M, Naura AS, Kim H, *et al.* ICAD deficiency in human colon cancer and predisposition to colon tumorigenesis: Linkage to apoptosis resistance and genomic instability. *PLoS One* 2013;8:e57871.
  29. Khan MS, Halagowder D, Devaraj SN. Methylated chrysin, a dimethoxy flavone, partially suppresses the development of liver preneoplastic lesions induced by N-nitrosodiethylamine in rats. *Food Chem Toxicol* 2011;49:173-8.
  30. Shine VJ, Anuja GI, Pradeep S, Suja SR. Molecular interaction of naringin and its metabolite naringenin to human liver fibrosis proteins: An *in silico* approach. *Phcog Mag* 2018;14:102-9.
  31. Chuli X, Yun D, Xiao T. Naringenin blocking signaling pathway PI3K/PKB inhibits human nasal epithelial cells secreting mucin MUC5AC. *Acta Med Mediterr* 2019;35:1379.
  32. Sak A, Wurm R, Elo B, Grehl S, Pöttgen C, Stüben G, *et al.* Increased radiation-induced apoptosis and altered cell cycle progression of human lung cancer cell lines by antisense oligodeoxynucleotides targeting p53 and p21(WAF1/CIP1). *Cancer Gene Ther* 2003;10:926-34.
  33. Chetty C, Bhoopathi P, Lakka SS, Rao JS. MMP-2 siRNA induced Fas/CD95-mediated extrinsic II apoptotic pathway in the A549 lung adenocarcinoma cell line. *Oncogene* 2007;26:7675-83.
  34. Chetty C, Bhoopathi P, Rao JS, Lakka SS. Inhibition of matrix metalloproteinase-2 enhances radiosensitivity by abrogating radiation-induced FoxM1-mediated G2/M arrest in A549 lung cancer cells. *Int J Cancer* 2009;124:2468-77.
  35. Inayat MS, Chendil D, Mohiuddin M, Eلفord HL, Gallicchio VS, Ahmed MM. Dioxid (a novel ribonucleotide reductase inhibitor) overcomes Bcl-2 mediated radiation resistance in prostate cancer cell line PC-3. *Cancer Biol Ther* 2002;1:539-45.
  36. Wan G, Mahajan A, Lidke D, Rajput A. Bcl-2 together with PI3K p110 $\alpha$  regulates cell morphology and cell migration. *Cell Death Dis* 2015;6:e2006.
  37. Trisciuglio D, Tupone MG, Desideri M, Di Martile M, Gabellini C, Buglioni S, *et al.* BCL-XL overexpression promotes tumor progression-associated properties. *Cell Death Dis* 2017;8:3216.
  38. Carné Trécesson S, Souzaé F, Basseville A, Bernard AC, Pécot J, Lopez J, *et al.* BCL-XL directly modulates RAS signalling to favour cancer cell stemness. *Nat Commun* 2017;8:1123.
  39. Xin M, Li R, Xie M, Park D, Owonikoko TK, Sica GL, *et al.* Small-molecule bax agonists for cancer therapy. *Nat Commun* 2014;5:4935.
  40. Sakakura C, Sweeney EA, Shirahama T, Igarashi Y, Hakomori S, Tsujimoto H, *et al.* Overexpression of bax enhances the radiation sensitivity in human breast cancer cells. *Surg Today* 1997;27:90-3.
  41. Roninson IB. Oncogenic functions of tumour suppressor p21(Waf1/Cip1/Sdi1): Association with cell senescence and tumour-promoting activities of stromal fibroblasts. *Cancer Lett* 2002;179:1-4.
  42. Zhang HM, Rao JN, Guo X, Liu L, Zou T, Turner DJ, *et al.* Akt kinase activation blocks apoptosis in intestinal epithelial cells by inhibiting caspase-3 after polyamine depletion. *J Biol Chem* 2004;279:22539-47.
  43. Santos NF, Silva RF, Pinto MM, Silva EB, Tasat DR, Amaral A. Active caspase-3 expression levels as bioindicator of individual radiosensitivity. *An Acad Bras Cienc* 2017;89:649-59.